ISSN 1028-334X, Doklady Earth Sciences, 2012, Vol. 444, Part 1, pp. 568–573. © Pleiades Publishing, Ltd., 2012.
Original Russian Text © K.A. Savko, V.V. Khiller, N.S. Bazikov, S.L. Votyakov, 2012, published in Doklady Akademii Nauk, 2012, Vol. 444, No. 3, pp. 289–295.

GEOLOGY

Th–U–Pb Age of Metamophism of the Vorontsovka Group Rocks, Voronezh Crystalline Massif, from Microbrobe Dating of Monazites

K. A. Savko[a], V. V. Khiller[b], N. S. Bazikov[a], and Academician S. L. Votyakov[b]

Received January 26, 2012

Abstract—The Paleoproterozoic metaterrigenous rocks of the Vorontsovka Group were studied. This series occupies a large area between the Precambrian crustal segments of the East European Craton, Sarmatia, and Volgo-Uralia. Based on the data of Th–U–Pb microprobe dating of monazites from the Vorontsovka Group, the age of zonal metamorphism is 2039 ± 26 Ma for the staurolite zone, 2015 ± 14 Ma for the muscovite–sillimanite zone, and 2008 ± 20 for the sillimanite–K-spar–cordierite zone. These data imply subsynchronity of the regional metamorphism and penetration of collision S-type granites of the Bobrov Complex about 2020 Ma B.P.

DOI: 10.1134/S1028334X12050194

Monazite is the mineral most often used in geochronometry for metamorphism dating, because it has a variable composition highly sensitive to changes in intensive and extensive parameters. Hence, it is an ideal geochronological sensor of metamorphic events. In the 1990s, the method of chemical electron-probe dating of U–Th-containing minerals was discovered [1]. A great number of publications has been devoted to application of this method for determination of the age of various geological objects (for example [2–4] and others).

The object of the present study is the Paleoproterozoic metaterrigenous rocks of the Vorontsovka Group. These rocks occupy a large area between the Precambrian crustal segments of the East European Craton, Sarmatia, and Volgo-Uralia, comprising more than 100 000 km^2 in area (Fig. 1). The thickness of deposits is 2–3 km in the southwest to 6–8 km in the east, based on the seismic data. In the sense of lithology, the series is very homogeneous and represents a stratum of metamorphized sandstone-schist flyschoid deposits. The absence of volcanic rocks in the Vorontsovka Group sections does not allow the formation age to be derived from igneous zircons. The previous study of zonal metamorphism for the Vorontsovka Group rocks identified and mapped the following zones: garnet (430–490°C), staurolite (490–520°C), staurolite–sillimanite (520–560°C), muscovite–sillimanite (560–600°C), sillimanite–K-feldspar–cordierite (600–750°C) [5]. The pressure of metamorphism is 3 to 5 kbar.

[a] *Voronezh State University, Voronezh, Russia*
e-mail: ksavko@geol.vsu.ru
[b] *Zavaritskii Institute of Geology and Geochemistry, Ural Branch, Russian Academy of Sciences, Yekaterinburg, Russia*

The U–Pb concordant isotope age of metamorphism, determined on the basis of the zircon monofraction from schists of the muscovite–sillimanite zone, is 2104 ± 4 Ma, while the age of piercing S-type granites is 2022 ± 8 Ma [6]. According to these data, metamorphism and folding in the Vorontsovka Group preceded the collision magmatism; this contradicts the known geodynamic models of evolution of the Precambrian folded zones. To solve this problem, we tried to estimate the metamorphism age of Vorontsovka Group rocks based on monazite. Monazite starts to occur in the uppermost greenschist facies, and its stability interval broadens as temperature increases, including the granulite facies [7].

Technique. We took the largest monazites from core samples of metapelites from different metamorphism zones (Fig. 1). Dating was performed by the Th–U–Pb method on a Cameca SX 100 microprobe at the Institute of Geology and Geochemistry (Ural Branch, Russian Academy of Sciences). The search for and identification of monazite grains in thin sections were made by their BSE images and energy-dispersive spectra; element mapping of grains was based on the measured intensity of the peak and background. The detection limits of ThO_2, UO_2, and PbO in monazite were 170, 65, and 73 ppm, respectively. Imaging was made at an accelerating power of 15 kV, and the beam current was 240 nA. The time of peak intensity measurement for Th, U, and Pb was 400 s, while it was 10 s for other elements and twice less for the background. The errors in the element content determination were the following: $\Delta Th/Th = 3.1–3.2$, $\Delta U/U = 1.9–9.5$, $\Delta Pb/Pb = 1.9–2.7$ relative %. Calculation of the monazite age was made with the use of original software [4] in terms of two alternative approaches: based on singular determinations of the contents of U, Th, and Pb at the point of the mineral's grain [2] and from Th/Pb–U/Pb pseudoisochrone [3].

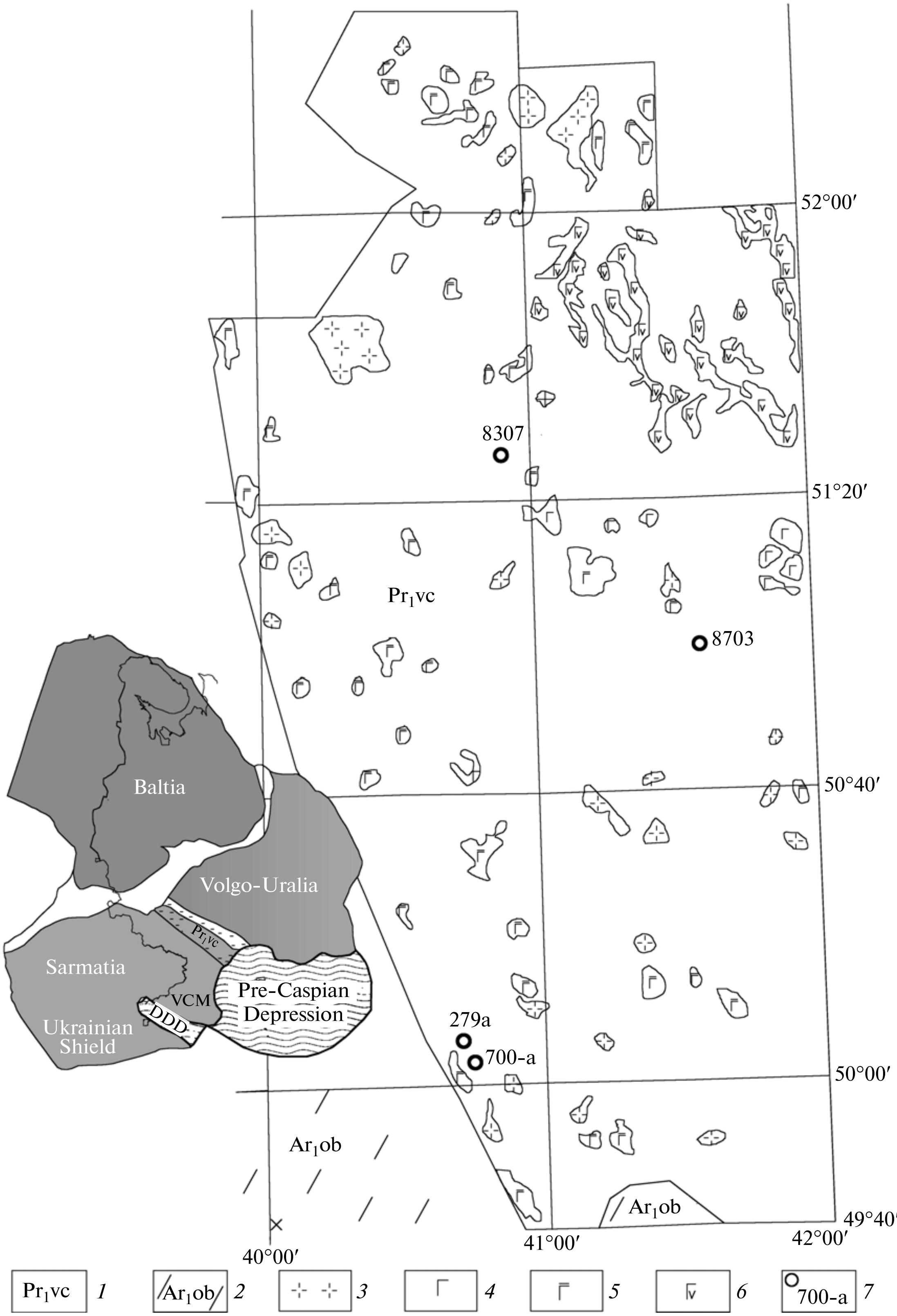

Fig. 1. The schematic geological map of the east part of the Voronezh Crystalline Massif, 1 : 1 000 000. (*1*) Metaterrigenous rocks of the Vorontsovka Group; (*2*) gray gneisses of the Rossosh Block and Varvarino Salient; (*3*) granites of the Bobrov Complex; (*4*) norites of the Elan Complex; (*5*) gabbroids and hyperbasites of the Mamon Complex; (*6*) gabbro-dolerites of the Novogol'skii Complex; (*7*) the drillhole position and number. VCM is the Voronezh Crystalline Massif; DDD is the Dniepr–Don Depression.

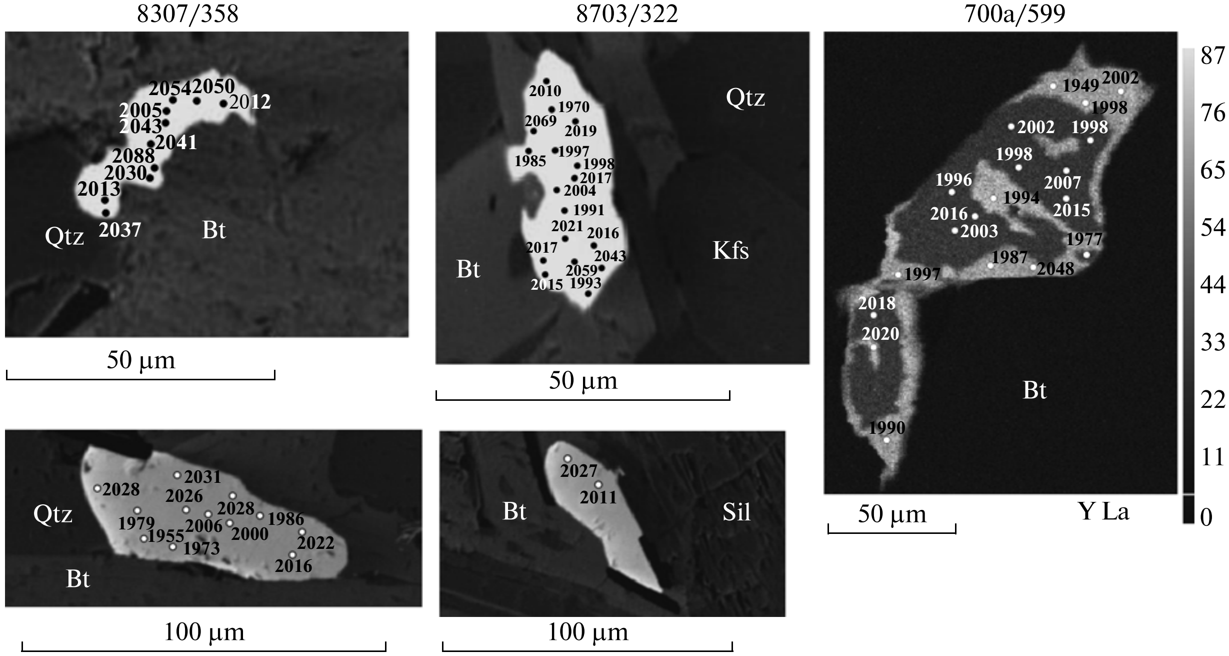

Fig. 2. Positions of dating points in monazite and the corresponding age values (Ma).

Staurolite zone. Monazite from sample 8307/358, taken for dating, was analyzed at ten points (Fig. 2). In terms of composition, the grain is not zonal; the ThO_2, UO_2, and PbO contents are 0.56–0.95, 0.58–0.79, and 0.28–0.34 wt %, respectively (see table). Based on the U, Th, and Pb contents, the monazite age was calculated by the method suggested in [2]; the values of 2005 to 2088 Ma were derived (table, Fig. 2), the weighted average value was 2037 ± 50 Ma, and the rms deviation was 0.096 (Fig. 3). The weighted average age calculated through the advanced technique [3] with the help of the Th/Pb–U/Pb diagram was 2039 ± 26 Ma, and the rms deviation was 0.38 (Fig. 3).

Muscovite–sillimanite zone. To determine the age, the elongated grain taken from garnet—sillimanite–biotite–muscovite gneiss (sample 8703/322) was analyzed at 17 points (Fig. 2). The thorium contents demonstrate a broad interval of values (1.92–4.16 wt % of ThO_2), but there are no regularities of its distribution in the grain. The ThO_2 concentrations here are 2–4 times greater than in monazite from the staurolite zone. The UO_2 and PbO concentrations are significantly lower than that of ThO_2 (0.36–0.67 and 0.32–0.58, respectively) and also do not reveal any regularities in distribution. In some samples from the muscovite–sillimanite zone, monazite grains contain yttrium-enriched narrow edges.

The age was calculated for 17 points, and the derived values ranged from 1970 to 2069 Ma, the weighted average value was 2013 ± 43 Ma, and the rms deviation was 0.073 (table, Figs. 2, 3). In the case of age calculation with the help of the Th/Pb–U/Pb diagram, the derived values were close (2015 ± 14 Ma), and the rms deviation was 0.30 (Fig. 3).

Sillimanite–K-feldspar–cordierite zone. The Th–U–Pb chemical dating of monazites was made for the samples 700a/599 and 279a/470.9 taken from garnet–sillimanite–cordierite gneisses (Fig. 1). Monazite from sample 700a/599 has a zonal structure (Fig. 2). The central and marginal parts of the crystal are different in terms of the Y and U contents; however, they have a close Th content. The yttrium concentration in the central zone is high (2.3–3.3 wt % of Y_2O_3), and the uranium one is lower (0.13–0.23 wt % of UO_2). In the marginal zone, the yttrium concentration decreases to 0.86–0.99 wt % of Y_2O_3, while that of uranium increases to 0.54–0.68 wt % of UO_2.

From the determined U, Th, and Pb contents at the points, we calculated the monazite age: 1949 to 2048 Ma (table), the weighted average age was 2002 ± 42 Ma, and the rms deviation was 0.040 (Figs. 2, 3). In the high- and low-yttrium zones, age values at the points lie within the limits of measurement error; therefore, there is no reason to distinguish the central and peripheral zones in terms of age. In the Th/Pb–U/Pb diagram (Fig. 3), the weighted average age value is 2004 ± 19 Ma (rms deviation is 0.15), which is comparable to the weighted average value of 2002 ± 42 Ma but with less error.

In sample 279a/470.9 we analyzed two small monazite grains. The larger elongated grain of 30 × 60 μm in size, in association with quartz and biotite, was analyzed at 12 points; the smaller one, in contact with sillimanite and biotite, at two points (Fig. 2). In contrast

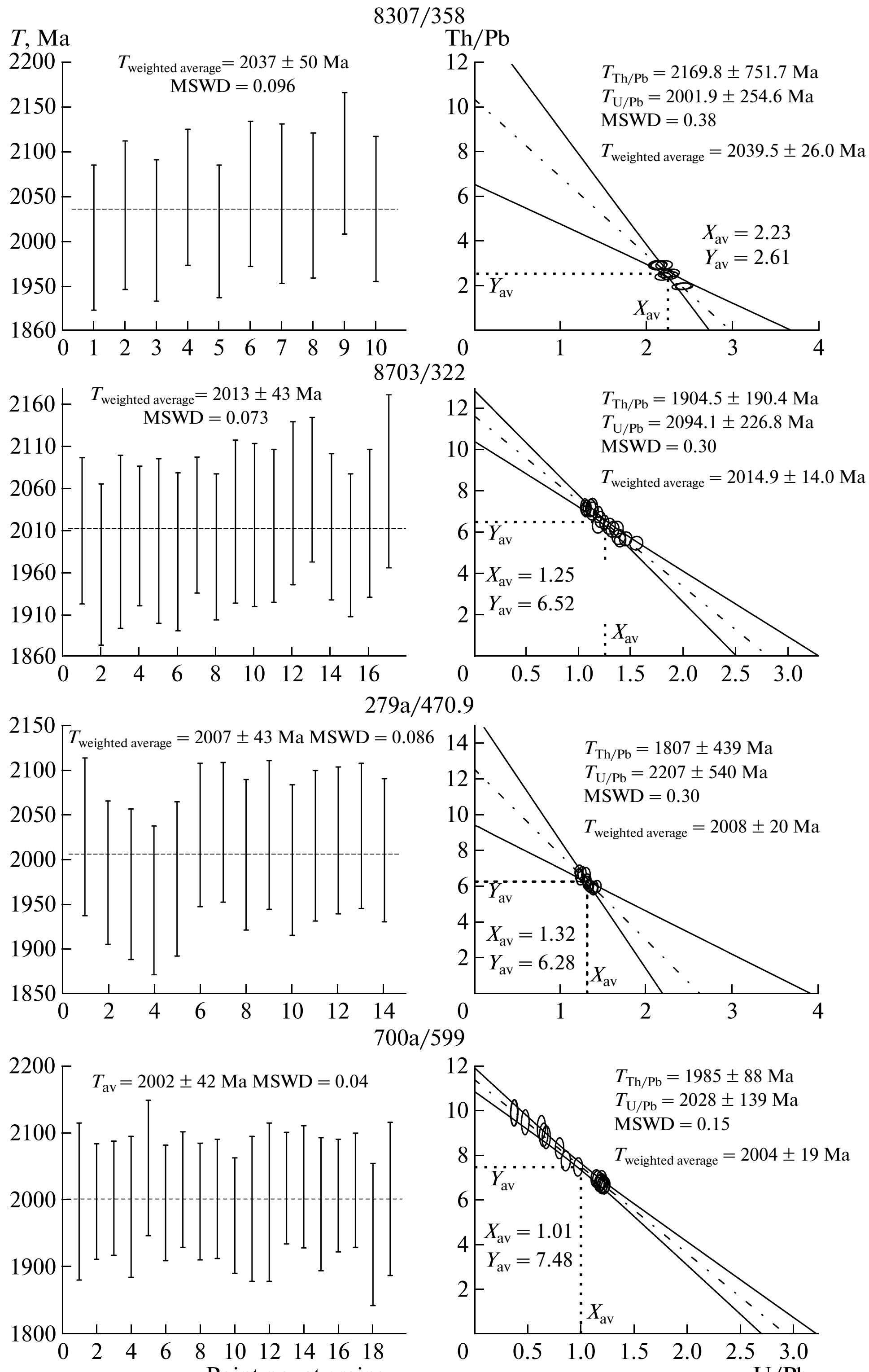

Fig. 3. Variations in monazite ages calculated based on singular points and the value of the weighted average age after [2] and based on the Th/Pb–U/Pb diagrams [3].

to monazite from sample 700a/599, a clear zoning in terms of Y and U contents was not found.

Based on the U, Th, and Pb contents determined at points, the age values from 1955 to 2028 Ma were derived (table), the weighted average value was 2007 ± 43 Ma, and the rms deviation was 0.086 (Fig. 3). From the calculation made with the help of the Th/Pb–U/Pb diagram, a weighted average value with less error

Th, U, and Pb contents in the monazite and age values calculated for the points by the method from [2]

Point	Content, ppm			Standard deviation, ppm			Rel. error, %			Age, Ma	Error, Ma
	ThO_2	UO_2	PbO	ThO_2	UO_2	PbO	ThO_2	UO_2	PbO		
8307/358											
1	9186	6815	3095	330	96	77	3.59	1.41	2.49	2005	81
2	5607	6672	2775	234	96	74	4.17	1.44	2.67	2030	83
3	8082	7066	3097	300	97	77	3.71	1.37	2.49	2013	79
4	8797	7576	3408	319	100	79	3.63	1.32	2.32	2050	76
5	6543	7850	3224	258	101	78	3.94	1.29	2.42	2012	74
6	9502	6756	3197	339	96	78	3.57	1.42	2.44	2054	81
7	8094	5830	2732	300	92	75	3.71	1.58	2.75	2043	89
8	9502	6891	3219	339	97	78	3.57	1.41	2.42	2041	81
9	8121	7220	3299	301	98	79	3.71	1.36	2.39	2088	79
10	7504	6789	2997	283	96	75	3.77	1.41	2.50	2037	81
8703/322											
1	37133	5384	5104	1165	87	93	3.14	1.62	1.82	2010	87
2	26498	4105	3646	842	82	82	3.18	2.00	2.25	1970	96
3	22394	3565	3162	719	80	78	3.21	2.24	2.47	1997	103
4	41625	6225	5767	1301	91	99	3.13	1.46	1.72	2004	83
5	19629	4298	3163	636	84	78	3.24	1.95	2.47	1998	98
6	28628	4410	3966	907	84	84	3.17	1.90	2.12	1985	94
7	35346	6742	5425	1111	94	96	3.14	1.39	1.77	2017	81
8	31478	5383	4553	993	88	89	3.15	1.63	1.95	1991	87
9	20533	4380	3315	663	84	79	3.23	1.92	2.38	2021	97
10	21275	4316	3352	685	83	79	3.22	1.92	2.36	2017	97
11	27254	4911	4082	865	86	85	3.17	1.75	2.08	2016	91
12	19170	4547	3292	623	85	79	3.25	1.87	2.40	2043	97
13	24415	5997	4302	780	92	87	3.19	1.53	2.02	2059	86
14	36463	5403	5065	1145	88	93	3.14	1.63	1.84	2015	87
15	21336	5979	3863	688	92	84	3.22	1.54	2.17	1993	85
16	22313	5632	3893	717	90	84	3.21	1.60	2.16	2019	88
17	20744	3842	3239	670	82	79	3.23	2.13	2.44	2069	103
279a/470.9											
1	29700	5663	4580	943	94	91	3.17	1.65	1.99	2026	88
2	29547	6987	4900	935	97	91	3.17	1.38	1.86	1986	80
3	31651	5875	4682	999	91	90	3.16	1.55	1.91	1973	84
4	30944	5995	4613	978	91	89	3.16	1.52	1.93	1955	83
5	31118	5546	4544	983	90	88	3.16	1.62	1.95	1979	86
6	29670	6998	5036	939	97	92	3.17	1.38	1.83	2028	80
7	34264	7618	5669	1078	100	98	3.15	1.31	1.73	2031	78
8	32877	6025	4930	1036	92	92	3.15	1.53	1.86	2006	84
9	29295	6411	4803	928	94	90	3.17	1.47	1.88	2028	83
10	30229	6215	4743	956	93	90	3.16	1.50	1.91	2000	84
11	29666	6247	4750	939	93	90	3.17	1.49	1.89	2016	84
12	31077	6554	4995	982	95	92	3.16	1.44	1.84	2022	82
13	29644	6929	5009	938	96	92	3.17	1.39	1.84	2027	81
14	29828	6927	4976	944	96	92	3.16	1.39	1.84	2011	80

Table. (Contd.)

Point	Content, ppm			Standard deviation, ppm			Rel. error, %			Age, Ma	Error, Ma
	ThO_2	UO_2	PbO	ThO_2	UO_2	PbO	ThO_2	UO_2	PbO		
700a/599											
1	34052	1292	3435	1072	67	78	3.15	5.20	2.26	1998	117
2	33779	6213	5052	1063	117	90	3.15	1.88	1.79	1998	86
3	34867	6271	5180	1096	118	91	3.14	1.87	1.75	2003	85
4	34279	2638	3886	1079	81	81	3.15	3.08	2.08	1990	105
5	32132	3572	4137	1014	91	84	3.16	2.55	2.04	2048	101
6	34827	6113	5105	1095	116	91	3.15	1.89	1.77	1996	86
7	35390	6157	5227	1112	117	91	3.14	1.90	1.75	2016	86
8	34292	5743	4940	1079	112	89	3.15	1.94	1.80	1998	87
9	32816	5395	4703	1034	108	88	3.15	2.01	1.87	2002	89
10	34295	5914	4938	1079	114	89	3.15	1.92	1.81	1977	86
11	31920	2341	3574	1007	78	79	3.15	3.32	2.21	1987	108
12	32642	1252	3294	1028	66	76	3.15	5.30	2.31	1997	118
13	37456	6785	5629	1175	123	93	3.14	1.81	1.66	2018	83
14	36610	4780	4884	1149	101	88	3.14	2.11	1.79	2020	91
15	34775	3356	4175	1093	87	82	3.14	2.60	1.97	1994	99
16	35042	6447	5269	1101	119	91	3.14	1.85	1.73	2007	84
17	35661	6250	5279	1120	117	91	3.14	1.87	1.72	2015	85
18	33623	2299	3632	1058	78	79	3.15	3.38	2.17	1949	106
19	32756	1663	3451	1032	72	77	3.15	4.32	2.24	2002	114

was derived, 2008 ± 20 Ma (Fig. 3); this value is very close to that derived for monazite from sample 700a/599 of the same sillimanite–K-spar–cordierite zone. Nearly the same age values derived for monazites from the Vorontsovka Group rocks, taken in places spaced nearly by 300 km, verify their own validity.

Accumulation of thick strata of terrigenous deposits of the Vorontsovka Group took place in the interval of 2200–2100 Ma owing to washing-out of the continental crust of the Volgo-Uralian segment [8]. The concordant age of clastogenic zircons from biotite–muscovite gneisses of the Vorontsovka Group varies from 2129 ± 15 to 2208 ± 22 Ma (SHRIMP II, VSEGEI, St. Petersburg; unpublished data by A.V. Samsonov and A.N. Larionov). Therefore, the age of metamorphism determined based on zircon monofractions [6] is 2104 ± 4 Ma and very close to the age estimates for detrital zircons. The problem of the zircon-based metamorphism age determination is related to the degree of integrity of either detrital zircons proper, or their cores with edges recrystallized during metamorphism.

Thus, the age of zonal metamorphism for the Vorontsovka Group rocks is 2039 ± 26 Ma for the staurolite zone, 2015 ±14 Ma for the muscovite–sillimanite zone, and 2008 ± 20 for the sillimanite–K-feldspar–cordierite zone. These data imply subsynchronity of the regional metamorphism and penetration of collision S-type granites of the Bobrovka Complex about 2020 Ma B.P.

ACKNOWLEDGMENTS

This study was supported by the Russian Foundation for Basic Research (project nos. 09–05–00513 and 09–05–00821) and by the Federal Targeted Program "Scientific-Pedagogical Personnel of Innovative Russia 2009–2013" (state contract no. 02.740.11.0727).

REFERENCES

1. K. Suzuki, M. Adachi, and T. Tanaka, Sedim. Geol. **75**, 141–147 (1991).
2. J. M. Montel, S. Forest, M. Veschambre, et al., Chem. Geol. **131**, 37–53 (1996).
3. A. Cocherie and F. Albarede, Geochim. Cosmochim. Acta **65**, 4509–4522 (2001).
4. S. L. Votyakov, V. V. Khiller, Y. V. Shchapova, and A. V. Porotnikov, Litosfera, No. 4, 94–115 (2010).
5. K. A. Savko and Yu. V. Gerasimov, Tr. NIIIG Voronezh. Univ., No. 8, p. 131.
6. E. V. Bibikova, S. V. Bogdanova, A. V. Postnikov, et al., Stratigr. Geol. Correl. **17**, 561–573 (2009) .
7. K. A. Savko and N. S. Bazikov, Petrology **19**, 445–469 (2011).
8. K. A. Savko, A. V. Samsonov, and N. S. Bazikov, Vestn. Voronezh. Univ. Ser. Geol., No. 1, 70–94 (2011).